

## A two-stage heating scheme for heat assisted magnetic recording

Shaomin Xiong, Jeongmin Kim, Yuan Wang, Xiang Zhang, and David Bogy

Citation: *Journal of Applied Physics* **115**, 17B702 (2014); doi: 10.1063/1.4853275

View online: <http://dx.doi.org/10.1063/1.4853275>

View Table of Contents: <http://scitation.aip.org/content/aip/journal/jap/115/17?ver=pdfcov>

Published by the AIP Publishing

---

### Articles you may be interested in

**Analysis of signal-to-noise ratio impact in heat assisted magnetic recording under insufficient head field**  
*J. Appl. Phys.* **117**, 17D133 (2015); 10.1063/1.4917004

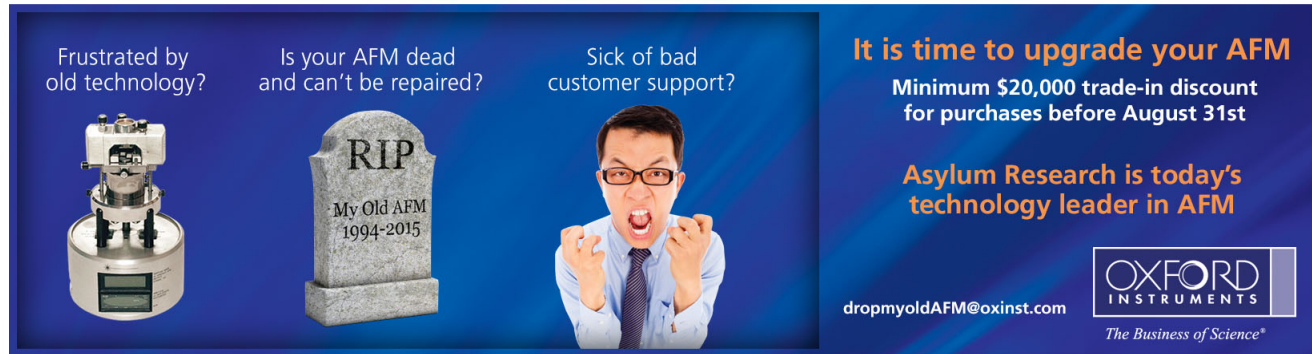
**Measurements of the write error rate in bit patterned magnetic recording at 100 – 320 Gb / in<sup>2</sup>**  
*Appl. Phys. Lett.* **96**, 052509 (2010); 10.1063/1.3304166

**Thermal effects of heated magnetic disk on the slider in heat-assisted magnetic recording**  
*J. Appl. Phys.* **99**, 08N102 (2006); 10.1063/1.2163323

**Pole tip protrusion of giant magnetic recording heads: Simulation and experimental verification**  
*J. Appl. Phys.* **97**, 10P303 (2005); 10.1063/1.1851672

**Demonstration and characterization of 130 Gb/in<sup>2</sup> magnetic recording systems**  
*J. Appl. Phys.* **93**, 6552 (2003); 10.1063/1.1540138

---



Frustrated by old technology?

Is your AFM dead and can't be repaired?

Sick of bad customer support?

RIP  
My Old AFM  
1994-2015

It is time to upgrade your AFM  
Minimum \$20,000 trade-in discount  
for purchases before August 31st

Asylum Research is today's  
technology leader in AFM

dropmyoldAFM@oxinst.com

OXFORD  
INSTRUMENTS

The Business of Science®

## A two-stage heating scheme for heat assisted magnetic recording

Shaomin Xiong,<sup>a)</sup> Jeongmin Kim, Yuan Wang, Xiang Zhang, and David Bogy  
*Department of Mechanical Engineering, University of California at Berkeley, Berkeley, California 94720, USA*

(Presented 7 November 2013; received 22 September 2013; accepted 3 October 2013; published online 2 January 2014)

Heat Assisted Magnetic Recording (HAMR) has been proposed to extend the storage areal density beyond 1 Tb/in.<sup>2</sup> for the next generation magnetic storage. A near field transducer (NFT) is widely used in HAMR systems to locally heat the magnetic disk during the writing process. However, much of the laser power is absorbed around the NFT, which causes overheating of the NFT and reduces its reliability. In this work, a two-stage heating scheme is proposed to reduce the thermal load by separating the NFT heating process into two individual heating stages from an optical waveguide and a NFT, respectively. As the first stage, the optical waveguide is placed in front of the NFT and delivers part of laser energy directly onto the disk surface to heat it up to a peak temperature somewhat lower than the Curie temperature of the magnetic material. Then, the NFT works as the second heating stage to heat a smaller area inside the waveguide heated area further to reach the Curie point. The energy applied to the NFT in the second heating stage is reduced compared with a typical single stage NFT heating system. With this reduced thermal load to the NFT by the two-stage heating scheme, the lifetime of the NFT can be extended orders longer under the cyclic load condition. © 2014 AIP Publishing LLC. [<http://dx.doi.org/10.1063/1.4853275>]

The magnetic recording based hard disk drive (HDD) plays a most critical role in mass data storage. The booming data market stimulates the industry to continuously increase the storage areal density. While scaling the areal density in magnetic recording, one must maintain the balance in media signal-to-noise (SNR), thermal stability, and writability. The magnetic grain is sometimes unable to keep its magnetic orientation when its size is reduced further in current perpendicular magnetic recording (PMR) technology, because the thermal fluctuation exceeds the energy barrier. Heat Assisted Magnetic Recording (HAMR<sup>1</sup>) was proposed to overcome those challenges and to permit the continued increase in areal density. In HAMR systems, a laser is used to locally heat the high anisotropy media to the Curie point (~400 °C) allowing the magnetic switching field to be reduced so that the writing process can be accomplished.

The size of the magnetic bit needs to be about 25 nm as the areal density keeps increasing further. The magnetic writing width highly depends on the size of the thermal profile on the disk surface in HAMR systems. A small heating area below the diffraction limit can be achieved by a near field transducer (NFT). The laser from a laser diode is delivered to the NFT structure on the air bearing surface. The light is further confined by the NFT to about 25 nm or less, depending on the design of the NFT. The NFT structure is usually made from some dielectric material and noble metal, such as gold. Even with the most efficient light delivery design, only a fraction of the laser power is absorbed by the media. A large fraction of the power is absorbed and dissipated around the NFT in the head and this leads to the overheating of the NFT. The temperature of the NFT can be

raised up to several hundred degrees Celsius and the extreme cyclic thermal load can result in the failure of the NFT after several tens of recording tracks,<sup>2</sup> which is far below the 5 yr warranty requirement of the commercial magnetic storage application.

To make the NFT more reliable in HAMR systems under millions of cycles, it is necessary to reduce the thermal load to the NFT structure while maintaining the amount of the total transmitted energy to the disk. In this work, we propose an approach to reduce the thermal load on the NFT by separating the NFT heating process into two stages. In the first stage, a laser waveguide structure is placed in front of the NFT. This waveguide transmits the laser energy to the disk surface and heats the disk to a peak temperature lower than the Curie temperature. Then, the NFT works as the second stage to heat a smaller area inside the large waveguide heated area further to reach the Curie point. The laser power input to each stage can be independently controlled in order to obtain an appropriate thermal profile for HAMR writing.

Here, we designed a bow-tie aperture structure as a NFT to focus light to a spot about 25 nm, using a commercial finite-difference time-domain (FDTD) software (CST microwave studio). A 3D finite element method (FEM) thermal model was developed to calculate the temperature increase of the media under the two heating sources, using ANSYS. The magnetic switching field of the magnetic layer was obtained from a Callen-Callen model for HAMR systems.<sup>3</sup>

Figure 1(a) shows a schematic diagram of the two-stage heating scheme. The waveguide is located in front of the NFT structure, with a spacing of d. Fig. 1(b) shows the typical laser intensity distribution on the disk surface from the waveguide, calculated from CST. The dimension of the intensity profile depends on the size of the Ta<sub>2</sub>O<sub>5</sub> core of the waveguide. The profile can be simplified to be a 2D

<sup>a)</sup>Author to whom correspondence should be addressed. Electronic mail: xshaomin@berkeley.edu.

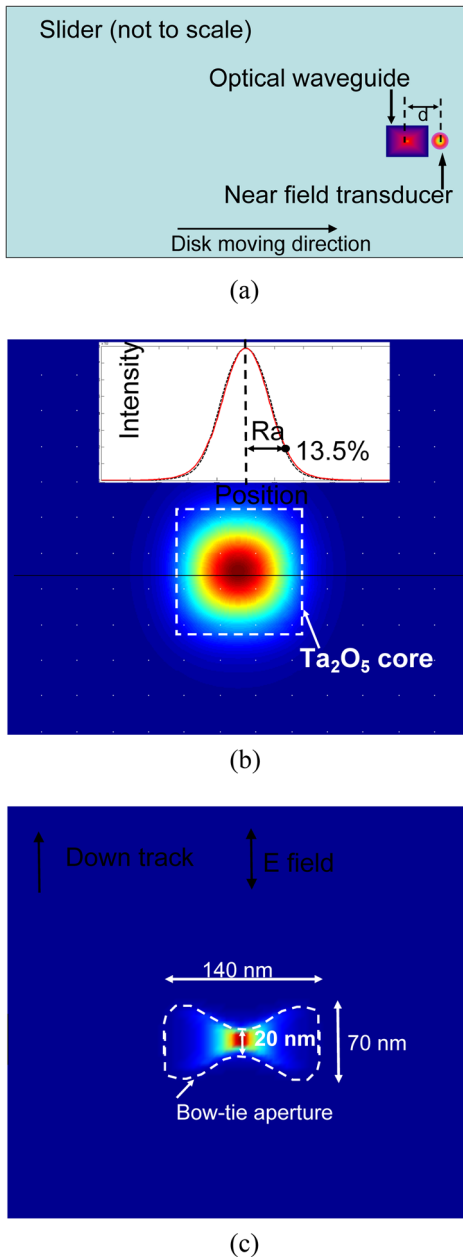


FIG. 1. (a) Schematic diagram of the two-stage heating slider; Laser intensity distributions for (b) the first stage heating by the waveguide and (c) the second stage heating by the NFT.

Gaussian distribution function. The radius ( $1/e^2$ ) of the laser intensity profile measured at the surface of the disk is  $R_a$ . Fig. 1(c) shows the absorbed power distribution on the surface of the disk from the NFT. The calculated intensity profile is close to a rectangular shape. The diameter of the profile ( $1/e^2$ ) along the down track direction is close to 25 nm which satisfies the requirement of HAMR systems.

The temperature distribution in the medium was calculated by solving the thermal diffusion equation using FEM in ANSYS. The absorbed power distributions described above were used as heat flux sources in the FEM thermal model. The disk has four layers with different thermal properties.<sup>4</sup> The mesh size is 25 nm by 50 nm in the x-y plane.

The switching field  $H_k$  of the magnetic layer relies on the thermal profile while the thermal distribution depends on

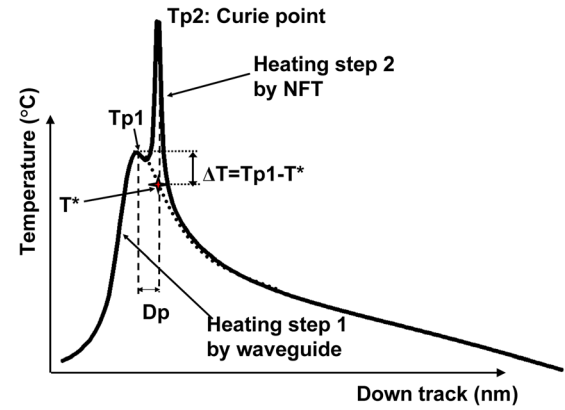


FIG. 2. A typical thermal profile on the media surface under the two heating stages.

the conditions of the heating sources, including the sizes of the two heating sources and the spacing between them. Fig. 2 shows a typical thermal profile for the two-stage heating scheme HAMR. The design goal is to heat a local small area of the magnetic layer to the media Curie point after combining the two heating stages. The waveguide heating can raise the disk background to a temperature lower than the Curie point; for example, it can raise the background to 200 °C. At this temperature, the magnetic bits in the adjacent tracks cannot be thermally erased by the waveguide heating. At the same time, the locations of the two peaks of the temperature profile under the two heating sources should be as close as possible. The distance between these two peaks is labeled  $D_p$  as shown in Fig. 2. The background temperature ( $T^*$ ) on the disk surface where the NFT heat is applied is always lower than the peak temperature ( $T_{p1}$ ) in the waveguide heating stage. This temperature difference is denoted as  $\Delta T$ , which can be eliminated when  $D_p$  is 0.  $D_p$  is determined by the sizes of the two heating sources and the physical spacing between them, which is denoted as  $d$  in Fig. 1(a). The size of the NFT heating source is constrained to be close to 25 nm because of the requirement of the high recording density. So  $D_p$  mainly depends on the size of the waveguide heating source ( $R_a$ ) in the first stage and on  $d$ .  $R_a$  is mainly controlled by the dimension of the waveguide and can be calculated using the CST microwave studio.

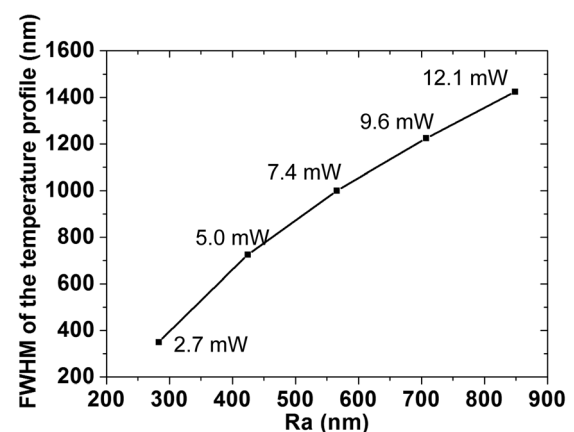


FIG. 3. FWHM of the temperature distribution in the waveguide heating stage by different laser radii ( $R_a$ ).

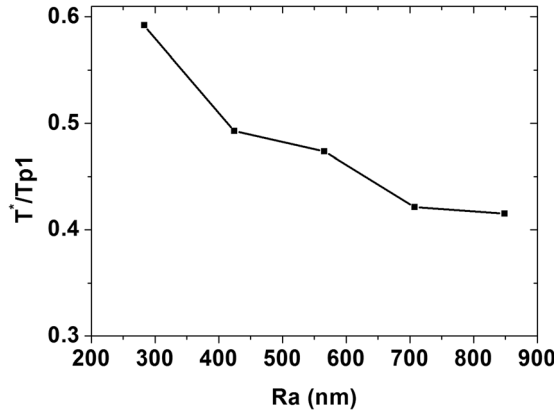


FIG. 4. Ratio of the background temperature  $T^*$  and peak temperature  $T_{p1}$  under different  $R_a$  in the waveguide heating stage.

The heating sources with different sizes from the waveguide generate different temperature distributions on the disk surface. Fig. 3 shows the full width at half maximum (FWHM) of the temperature profile on the magnetic layer and the power needed to heat the disk close to  $200^\circ\text{C}$  when the disk speed is  $20\text{ m/s}$ . More energy is consumed to heat a larger area to  $200^\circ\text{C}$  and the width of the temperature profile is larger. When a larger  $R_a$  is used, more adjacent tracks will be heated and affected.

There is another trade-off between  $R_a$ ,  $\Delta T$ , and  $d$ . Smaller  $R_a$  can provide a sharper thermal gradient which is better for HAMR writing,<sup>1</sup> but leads to more changes in  $\Delta T$ . It is possible that overheating of the magnetic bits happens at the location of the temperature peak in the waveguide heating if  $R_a$  is small and the power input is large. If a larger  $R_a$  is used, a larger size waveguide structure should also be used. In this case, the physical spacing between the heating sources should be increased to avoid the interference between the two heating sources. Then  $D_p$  is increased and  $\Delta T$  becomes larger again. Fig. 4 shows the ratio of the background temperature  $T^*$  and  $T_{p1}$  in the waveguide heating as  $R_a$  changes. It is seen that the ratio decreases as the waveguide heating becomes larger.

The Callen-Callen model predicts the magnetic switching field distribution of the magnetic layer for this two-stage heating scheme, as shown in Fig. 5. The red curve shows the switching field if only the NFT heating source is applied as in the currently proposed single stage HAMR systems. The gradients of the switching field at the valley of the two curves are at the same order for both HAMR heating schemes. So the two-stage heating scheme can have similar writing capability as the single NFT scheme, but it can have better reliability because the thermal load to the NFT is reduced. In this simulation, the thermal load to the NFT is reduced by 30% in the two-stage heating scheme compared with the single stage heating system. Thus, it is expected that

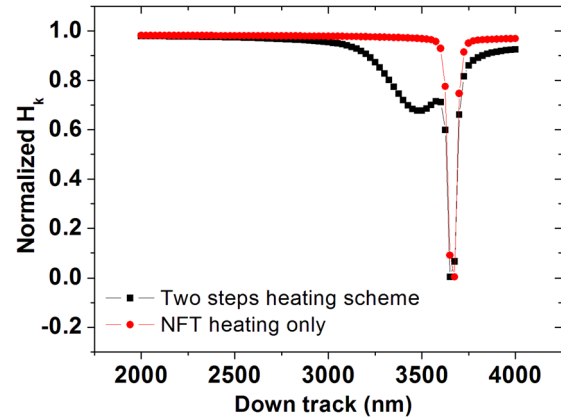


FIG. 5. Switching field  $H_k$  distribution on the disk surface for the two-stage heating scheme and single NFT heating scheme.

the temperature of the NFT and thermal stress in the NFT could be reduced as well for this two-stage heating scheme. However, great care should be taken for the two-stage heating scheme because the high background temperature could lead to adjacent track interference and erasure. Further optimization of the magnetic writer design could help to address this problem. The power inputs to the two stages can be controlled and balanced in order to get a good reliability and writing performance.

A two-stage heating scheme for the HAMR system is proposed in this work. The first stage provides a background temperature of about  $200^\circ\text{C}$  by use of an optical waveguide, which is about half of the temperature increase needed to reach the Curie point, while the NFT heats the media further to the Curie point. Numerical simulation shows that the distance between the two heating sources and the size of the waveguide source affect the performance of the two-stage heating scheme. The two-stage heating scheme can provide an effective writing performance for HAMR while the thermal load to the NFT is reduced compared to a single stage approach. So it is expected that the two-stage heating scheme can help to extend the lifetime of the NFT under the cyclic load condition.

This research was supported by NSF Nano-scale Science and Engineering Center (NSEC) for Scalable and Integrated Nanomanufacturing (SINAM) (Grant No. CMMI-0751621) and Computer Mechanics Laboratory (CML) of University of California, Berkeley.

<sup>1</sup>M. H. Kryder *et al.*, Proc. IEEE **96**, 1810 (2008).

<sup>2</sup>W. A. Challener *et al.*, Nat. Photonics **3**, 220 (2009).

<sup>3</sup>Shaomin Xiong and David Bogy, IEEE Trans. Magn., doi: 10.1109/TMAG.2013.2290760.

<sup>4</sup>ASTC Technical Documents, “ASTC HAMR reference media stack for NFT modeling,” (The International Disk Drive Equipment and Materials Association, 2011), [http://idema-cloud.smartsite.net/?page\\_id\\_2269](http://idema-cloud.smartsite.net/?page_id_2269).